ELSEVIER

Soil Dynamics and Earthquake Engineering 19 (2000) 551–558

SOIL DYNAMICS AND EARTHQUAKE ENGINEERING

www.elsevier.com/locate/soildyn

A time-domain viscous damping model based on frequency-dependent damping ratios

Der-Wen Chang[a,*], J.M. Roesset[b], Chan-Hua Wen[c]

[a]*Department of Civil Engineering, Tamkang University, Tamsui, Taiwan 25137, ROC*
[b]*Department of Civil Engineering, Texas A&M University, College Station, TX 77845, USA*
[c]*Graduate Research Assistant, Department of Civil Engineering, Tamkang University, Tamsui, 25137 Taiwan, ROC*

Accepted 13 August 2000

Abstract

This paper introduces the mathematics and procedures used in developing a time-dependent damping model for integration analyses of structural response. To establish the time-dependent viscous damping model, frequency-dependent damping ratios of the structure under a series of steady-state unit impulses corresponding to actual loads are first calculated. For simplicity, the ratios can be incorporated with the static stiffness of the structure to model approximately the impulse induced damping spectrum. According to the nature of the problem, these ratios can be calculated from the theoretical impedance functions and experimental observations. With the computed damping spectrum, the damping coefficient in the time domain can be obtained with the Fourier transform technique. Adopting the impulse–response method, the damping can be modeled rationally through integration with changing loads. Numerical examples are presented to show the feasibility of this model while the transform criterion is satisfied.

Keywords: Time-domain integration; Damping coefficient; Fourier transform; Impulse–response method; Equivalent damping ratios; Impedance functions

1. Introduction

Damping, which dissipate energy, as the velocities of motion and strain are varied, is important to dynamic structural analyses. Discussions of the possible damping models can be found in the literature: Refs. [1–4]. Presuming that the structures are excited at small strain levels, two types of damping, i.e. viscous and hysteretic, are commonly discussed. These models can be related by the critical damping ratios (fraction of critical damping), ξ, and the damping ratios (energy ratio), D, of the structure at different vibration modes, which yields:

$$\xi = D\omega_0/\omega \tag{1}$$

where ω is the excitation frequency of the structure (in rps), ω_0 is the fundamental frequency of the structure (in rps). Moreover, the equivalent viscous coefficient, C_{eq}, for a hysteretic structural system with damping ratio D can be expressed as:

$$C_{eq} = 2DK/\omega \tag{2}$$

where K is the structural stiffness. For certain analyses, the frequency dependence of the structural stiffness and the damping ratio are sometimes ignored to simplify the solution. In design practice, the damping coefficient can be modeled using Rayleigh damping and its alternatives. Considering the orthogonality of the modal shapes and the associated damping ratios, the mass M and the stiffness K of the structure can be used to model the viscous coefficient C as that defined in Rayleigh damping:

$$C = \alpha M + \beta K \tag{3}$$

where $\alpha = \xi\omega$ and $\beta = \xi/\omega$.. For easy applications, it is often assumed that the critical damping ratios ξ and the damping ratios D are the same for the frequencies of interest. The resolved solutions would be acceptable if the frequency effects were not significant. This model can be further considered in the time-domain analysis, presuming that the fundamental frequency and a stationary damping ratio can dominate the structural response. The ambiguity of the damping ratio treatment and the pre-processed modal analysis were shortcomings of this model. In the past few decades, the frequency-domain damping mechanism has been extensively investigated. A number of corresponding mathematical models were reported. A summary of the available damping models can be found in Ref. [5]. More recently, Makris and Constantinous [6] suggested a viscous

* Corresponding author. Tel./fax: +886-2-2623-4224.
E-mail address: dwchang@mail.tku.edu.tw (D.-W. Chang).

0267-7261/00/$ - see front matter
PII: S0267-7261(00)00072-5

damper following fractional calculus. This model can apply the frequency-dependent damping coefficient directly to the time-domain analysis. In order to control better the damping for time integration analyses, a number of studies [7–9] have proposed numerous time-dependent damping models to both specific and generalized engineering problems. These solutions are rather complicated in mathematics and have not been widely used in relevant analyses. To use the integration technique for the mechanical analyses, an alternative time-dependent damping model is proposed by Chang and Yeh [10] in modeling the pile response from direct wave equation analyses. In their work, a complex function of the time-dependent damping coefficient was suggested and the amplitudes of the functional were used in the analysis. For better physical interpretation of the model, the model is slightly revised, and applications of the model to both geometric and material dampings are discussed.

2. Theoretic procedures

For the equation of motion in time integration analysis, the damping force $F_d(t)$, at arbitrary time t, can be written as follows:

$$F_d(t) = C(t) \times V(t) \tag{4}$$

where $C(t)$ and $V(t)$ are the viscous damping coefficient and the velocity–time history at arbitrary time t. Considering many small time steps, the viscous coefficient $C(t)$ at a time stage can be assumed independent of $V(t)$, and to be affected mainly by the response history of the structure prior to that time. Applying the Fourier transform technique, a time-dependent viscous damping coefficient $C(t)$ can be expressed as:

$$C(t) = \frac{1}{2\pi} \int_{-\infty}^{\infty} C(\omega)\, e^{i\omega t}\, d\omega = \frac{1}{2\pi} \int_{-\infty}^{\infty} c(\omega) f(\omega)\, e^{i\omega t}\, d\omega \tag{5}$$

where $C(\omega)$ is the frequency-domain damping spectrum, $c(\omega)$ is the transfer function of the damping at unity steady-state excitations, and $f(\omega)$ is the loading spectrum associated with $F(t)$. Note that convolutions are required to obtain $C(\omega)$. Eq. (5) would be very difficult to solve if the loads last for a certain duration.

To simplify the above computations, the impulse–response method, in which the actual load–time history can be regarded as a continuous series of small impulses, is alternatively considered. The function $C(t)$ at arbitrary time t can then be expressed by:

$$C(t) = \int_{-\infty}^{t} c(t-\tau) F(\tau)\, d\tau \tag{6}$$

where τ is the applied time of the small impulses, $F(\tau)$ is the load applied at that time, and $c(t-\tau)$ is the decomposed damping at time t to a unit impulse applied at τ. For $\tau > t$, where the impulse does not exist, the upper limit of the integral can extend to infinity. This equation implies that the damping coefficient $C(t)$ can be obtained by integrating the decomposed damping function $c(t)$ to a set of unit impulses of the load–time history that is reproducible in the integration analysis. The decomposed damping function $c(t)$ due to the unit impulses can be computed from $c(\omega)$ using the Fourier transform. To reveal the mathematics, the integral of $F(t)$ with respect to the time between $(-\infty, \infty)$ is first present as a definite integral of the unit impulse function $\delta(t)$ and a constant parameter $\boldsymbol{I}$.

$$\int_{-\infty}^{\infty} F(t)\, dt = I \int_{-\infty}^{\infty} \delta(t)\, dt = I \times 1 \tag{7}$$

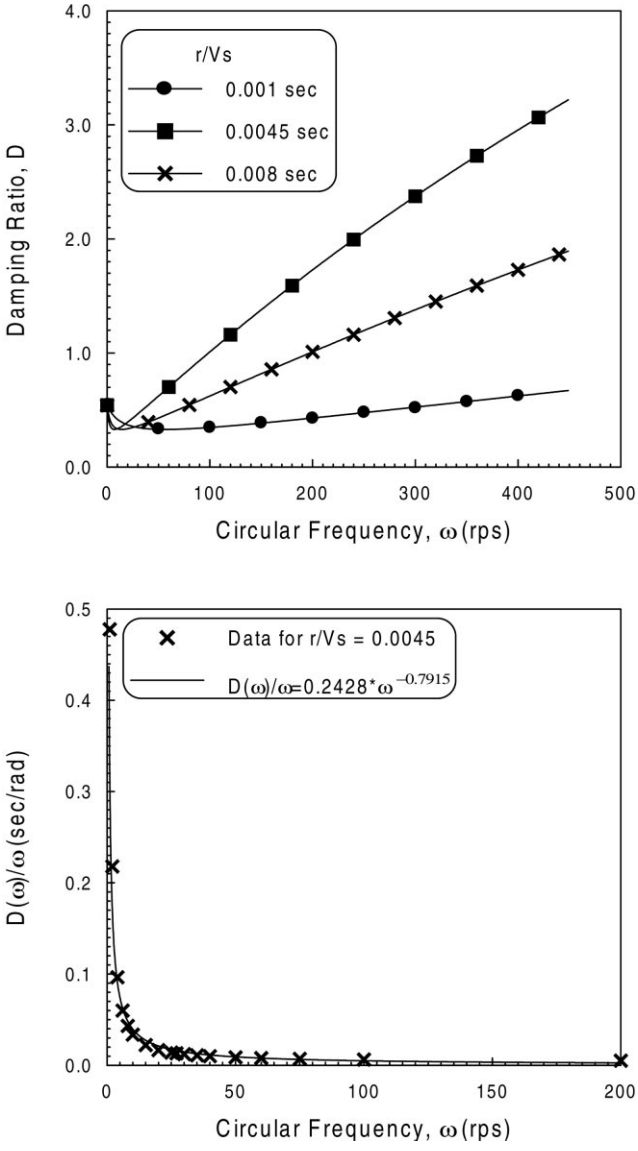

Fig. 1. Equivalent damping ratios of vertical soil impedance along pile shaft for single pile.

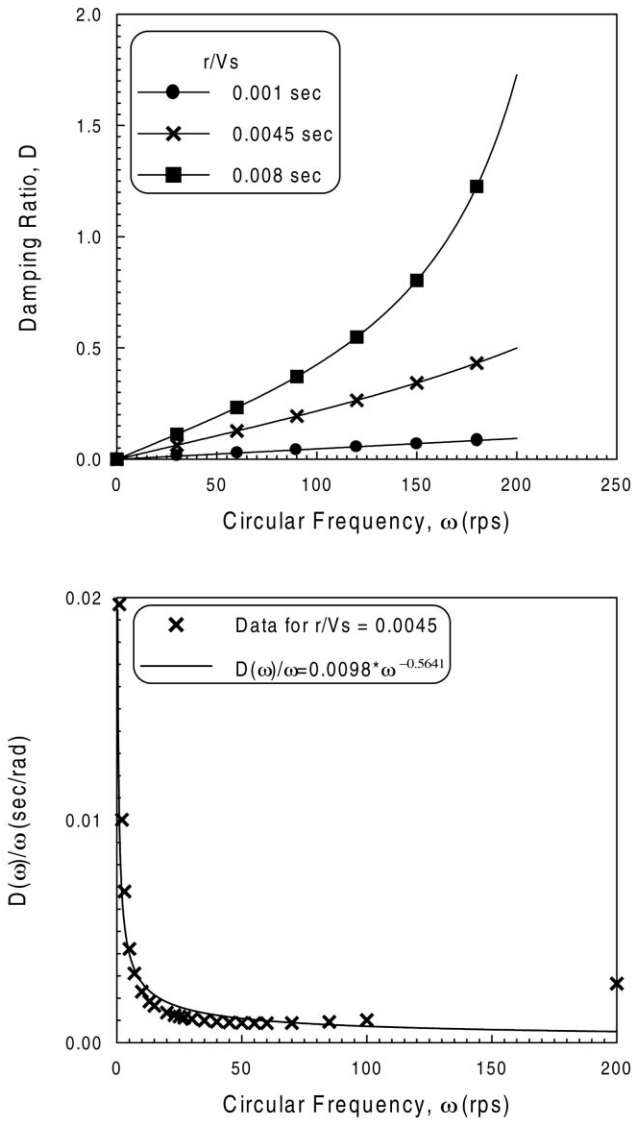

Fig. 2. Equivalent damping ratios of vertical soil impedance at pile tip for single pile.

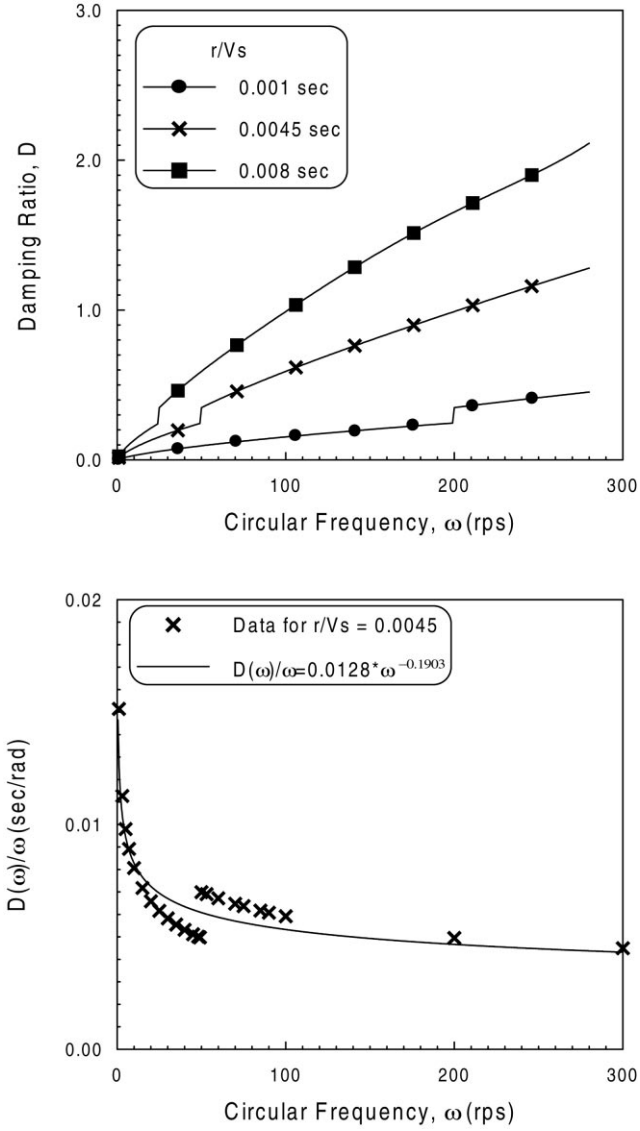

Fig. 3. Equivalent damping ratios of horizontal soil impedance along pile shaft for single pile.

The unit impulses $\delta(t)$ and their influences are constantly incorporated at various time steps of the analysis. Now recall that the result of the Fourier transform of $\delta(t)$ is:

$$h(\omega) = \int_{-\infty}^{\infty} \delta(t)\, e^{-i\omega t}\, dt = 1. \tag{8}$$

One may know that the unity-loads $h(\omega)$ are admissible in reproducing $c(\omega)$. Hence, the corresponding time-domain damping $c(t)$ can be calculated from the inverse Fourier transform on the convolutions of $c(\omega)$ and $h(\omega)$. Consequently, the expression can be written as:

$$c(t) = \frac{1}{2\pi} \int_{-\infty}^{\infty} c(\omega) h(\omega)\, e^{i\omega t}\, d\omega = \frac{1}{2\pi} \int_{-\infty}^{\infty} c(\omega)\, e^{i\omega t}\, d\omega. \tag{9}$$

Using the integration procedures presented in Eq. (6), one can solve for $c(t)$ easily at arbitrary time. Notice that this model is applicable to both material and geometric damping as long as $c(\omega)$ is suitable to the transform. This model can provide engineers with a physically time-dependent damping coefficient encountering the dynamic nature of the structure. It is also important to know that the velocity–time history is not required in deriving the coefficient; yet it can be used to substitute for the load time history $F(t)$ in Eq. (6) to attain the time history of the damping force, in stead of $C(t)$. In that case, one may use the same derivations to establish $c(t)$ while a series of unit impulse $\delta(t)$ and corresponding unity spectrum $h(\omega)$ are both present for the associated velocity influence. Certainly, to solve for the transfer damping function $c(\omega)$ of a linearly viscoelastic structural system, the equivalent damping ratios D need to be obtained first.

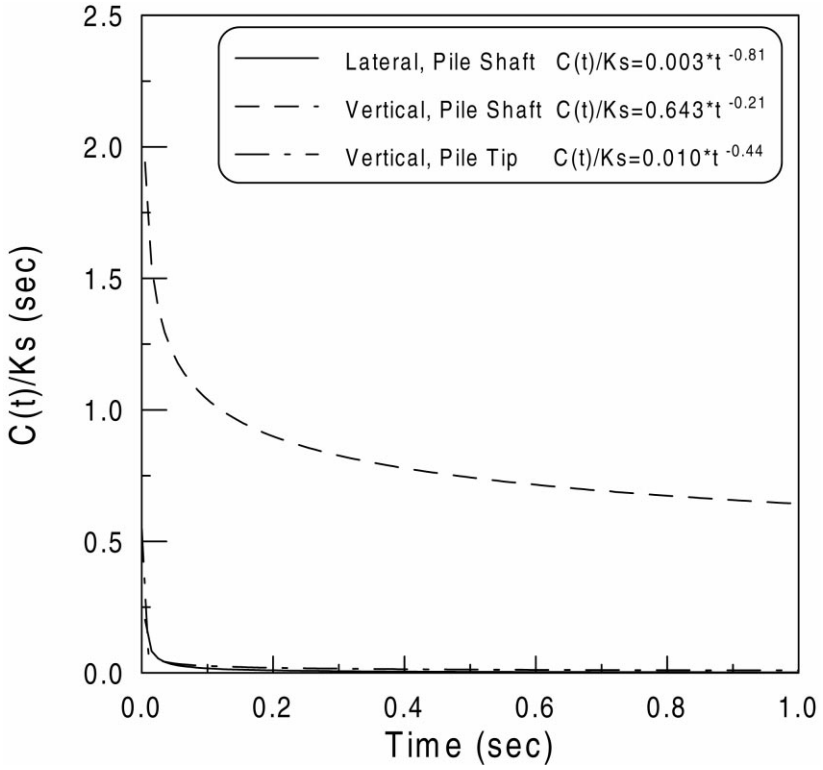

Fig. 4. Ratios between decomposed damping coefficient and soil stiffness against time for single pile.

3. Calculations for damping

3.1. Example of theoretical impedance functions

To establish the function $c(\omega)$, equivalent damping ratios calculated from the dynamic impedance functions K^* of a structure under unity steady-state loads are shown next. Recall that the equivalent damping ratios of the energy dissipation of a structural system can be computed as follows:

$$K^* = K_{\text{real}} + \mathrm{i}K_{\text{imag}} = K(\omega) + \mathrm{i}\omega C(\omega) \equiv K(\omega)\,(1 + 2\mathrm{i}D) \quad (10)$$

$$D \equiv \omega C(\omega)/2K(\omega) \quad (11)$$

where $K(\omega)$ and $C(\omega)$ are the stiffness and the damping of the structural impedance function, respectively. For simplicity, one may use the equivalent damping ratio and the 'static' structural stiffness K to reconstitute the dynamic impedance of the system. By assuming that the structure is excited under many unity steady-state loads $h(\omega)$, the transfer damping function $c(\omega)$, as appearing in Eq. (9), is as same as the function C_{eq} shown in Eq. (2). One can apply the available impedance functions to obtain these damping ratios. For example, the dynamic impedance functions, representing the soil resistance around a single pile under the steady-state excitations, have been used to model the associated damping ratios [10]. In that case, the available functions suggested by Novak [11] are: vertical soil impedance along pile shaft

$$K(\omega) + \mathrm{i}\omega C(\omega) = G(S_{w1}(a_0) + \mathrm{i}S_{w2}(a_0)), \quad (12)$$

vertical soil impedance at pile tip

$$K(\omega) + \mathrm{i}\omega C(\omega) = G\mathrm{r}(C_{w1}(a_0) + \mathrm{i}C_{w2}(a_0)) \quad (13)$$

horizontal soil impedance along pile shaft

$$K(\omega) + \mathrm{i}\omega C(\omega) = G(S_{x1}(a_0) + \mathrm{i}S_{x2}(a_0)), \quad (14)$$

where S_{w1}, S_{w2}, C_{w1}, C_{w2}, S_{x1} and S_{x2} are the transcendental functions of the non-dimensional frequency a_0 ($a_0 = r\omega/V_s$, where r is the pile radius and V_s is the shear wave velocity of the soils). According to Novak [11], these functions can be simplified for soils with various Poisson's ratios, and a_0 between 0 and 1.5.

Based on Eq. (11), the damping ratios of these impedance functions can be computed respectively. For piles having a radius of 0.3–0.8 m and located in soils with shear wave velocities of 90–250 m/s, the corresponding values of r/V_s are about 0.001–0.008 s. The damping ratios D at different r/V_s values against circular frequencies are plotted in Figs. 1–3. To conduct the transform, the values of $D(\omega)/\omega$ associated with the averaged r/V_s values (= 0.0045 s) can be fitted by regression analysis. For the ratios in the frequency ranges of interest, a simplified relationship found is:

$$D(\omega)/\omega = a\omega^{-b} \quad (15)$$

Parameters a and b are obtainable from the curve-fitting procedure. Substituting Eq. (15) into Eq. (2) with the static soil stiffness K, one can attain $c(\omega)$. To obtain a real function at time-domain, the damping spectrum is presumed symmetric to the ordinate. Hence the following equation

is different from the complex equation present in Ref. [10]. One can use the computer package 'Mathematica' [12] to derive the closed form solution.

$$c(t) = \frac{1}{2\pi}\int_{-\infty}^{\infty} c(\omega)h(\omega)\,e^{i\omega t}\,d\omega$$
$$= \frac{1}{2\pi}\int_{-\infty}^{\infty} 2Ka\omega^{-b}\,e^{i\omega t}\,d\omega$$
$$= \frac{2aKt^{(b-1)}\Gamma[1-b]\sin(0.5\pi b)}{\pi} = AKt^{-B} \qquad (16)$$

In the above equation, A and B are the damping model parameters. Function $\Gamma(z)$ denotes the Euler-Gamma function with variable z, and is equal to $\int_0^\infty t^{z-1}\,e^{-t}\,dt$; for positive integers n, $\Gamma(n) = (n-1)!$ Eq. (16) is newly suggested for physical damping and parameters A obtained for the cases of $r/V_s = 0.0045$ s are slightly different from those present in Ref. [10]. They were also comparable to the data points obtained from the FFT module FOUR2 suggested by Roesset and Kaussel [13]. The values of $c(t)$ over K against time, applicable to the vertically- and laterally-loaded pile analyses, are plotted in Fig. 4. The decomposed damping function $c(t)$ will decay as the time continues. This phenomenon indicates that soil damping can work effectively in the early periods of the response history. If a simple mathematical function of the modeled damping ratios is not available, one can use the

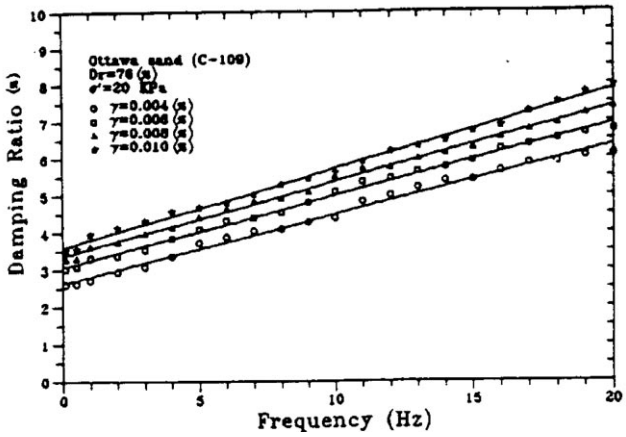

Fig. 5. Damping ratios vs frequency of Ottawa sand (from Ref. [19]).

module to compute the discrete data. Recently, Chang and Ou Yang, and Chang and Lin [14,15] have applied this model, with different soil stiffness, to wave equation analysis considering the pile interaction effects. Fig. 5 shows the discrete data of the transformed dampings for the center piles that are affected by the pile interactions in the 3×3 and 4×4 square-shaped pile groups, where $r/V_s = 0.0045$ s, $s/d = 3$ (s, pile-to-pile spacing; d, pile diameter) and soil damping ratio = 5%. It is interesting to know that the soil

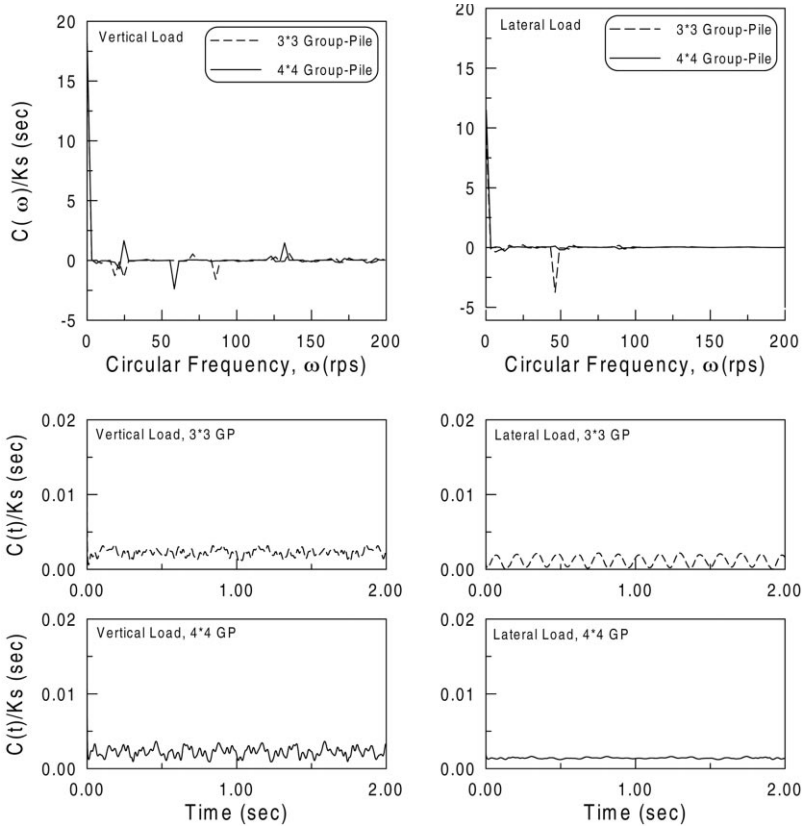

Fig. 6. Ratios between decomposed damping coefficient and soil stiffness against time for pile shaft interior pile in group-pile foundation.

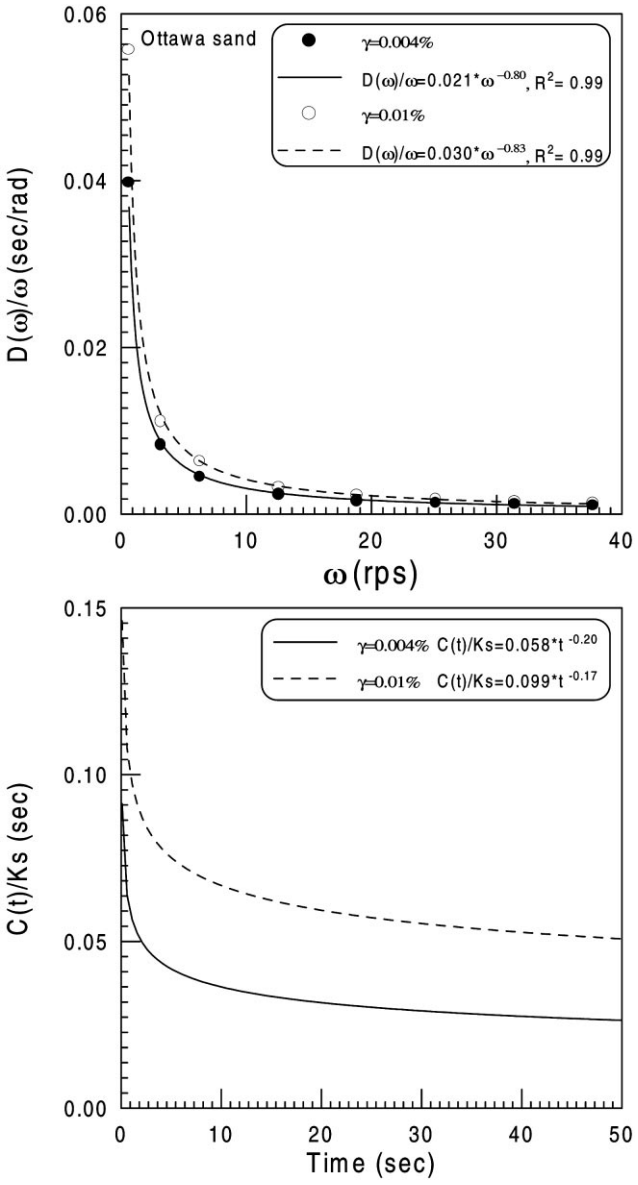

Fig. 7. Calculated material damping based on the data from Ref. [19].

dampings are approximately less than 0.5% of the soil stiffness (units — s) for the specific interactive piles.

3.2. Example from experimental observations

Damping coefficients obtained from material testing are discussed next. For soils at different conditions, Czakowski and Vinson [16], Isenhower and Stokoe [17], Sousa and Monismith [18], Lin et al. [19] and Bray et al. [20] have shown that the material damping ratios could depend on the frequency or the rate of the strain. Moreover, the possible frequency influences on the damping ratios are indeed different in various soils. According to the data from a series of cyclic-torsional-shear tests on Ottawa sand conducted by Lin et al. (Fig. 6), the internal damping of the soil at various strain levels were increased

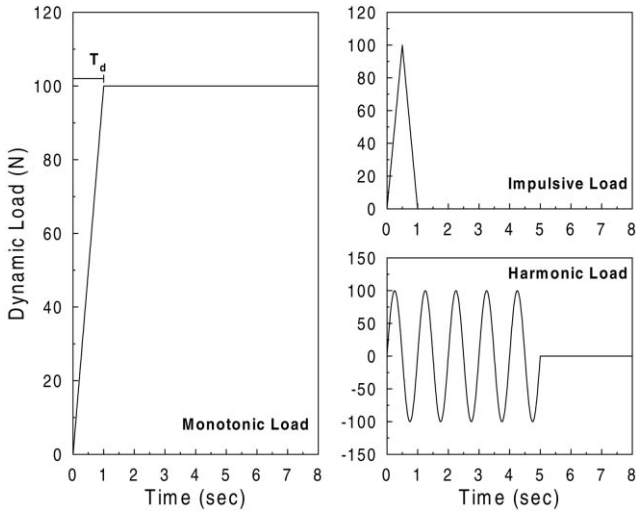

Fig. 8. Loading functions considered in numerical examples.

linearly between 2.5 and 8% with respect to the frequencies from 0.1 to 20 Hz. A modeling example is now conducted for these damping ratios with Eq. (15). Symmetry of the damping function is assumed to obtain the transformed solution. It is important to point out that the parameter b should be kept less than one in this case to obtain a rational damping coefficient. The functional of the resulted transformed coefficient will be less than zero as time increases for $b \geq 1$, which does not satisfy the physical nature of the vibrations. Fig. 7 illustrates the corresponding data and the available transform results.

In order to show the efficiency of the proposed model, structural response of an SDOF system, obtained from modeling with the calculated damping parameters, are compared with those obtained from the Rayleigh damping model. Parameters α and β in the Rayleigh damping model are computed as those occurring at resonance. Two and 5% material damping ratios are respectively considered for the simulations. The motion histories of the SDOF system, with dimensionless mass of one and dimensionless stiffness of 10, subjected to three different loads (as shown in Fig. 8) are examined. Notice that the time to reach the ultimate load in the monotonic loading case, and the duration of the impulse as well as the period of the 5-cycle harmonic loads, were termed T_d, and were set as 1, 1.98 and 5 s in the analyses. The comparative results for the response of the SDOF structure with a natural period, T_n, of 1.98 s are shown in Figs. 9–11. The results of this modeling were found compatible with those calculated from the Rayleigh damping. The differences of these two solutions are mainly caused by the estimated damping magnitude. For rapidly monotonic loading (whose structure's natural period is greater than T_d), the oscillations of the structure are pronounced. The

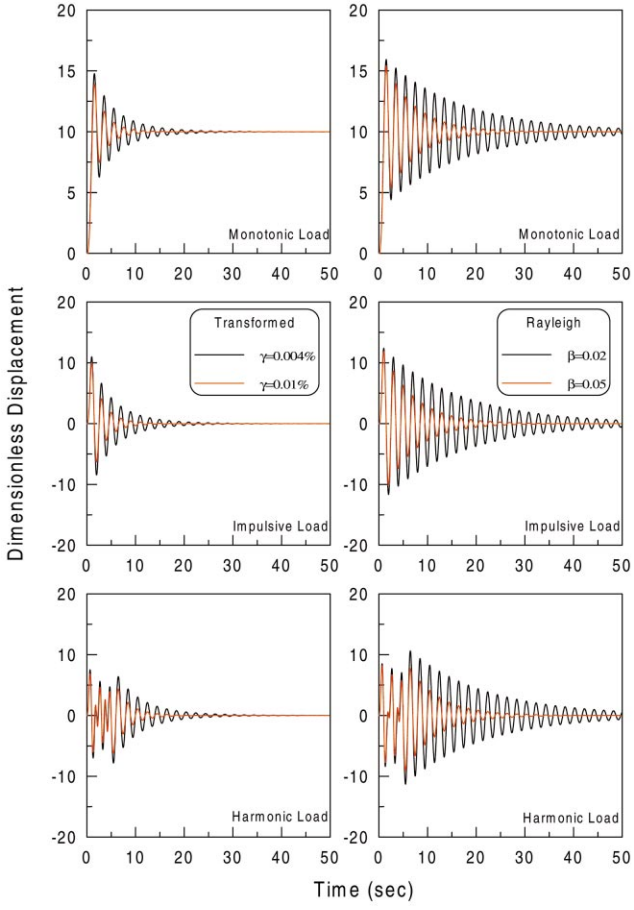

Fig. 9. Comparative SDOF structural response ($T_d = 1$ s $< T_n$).

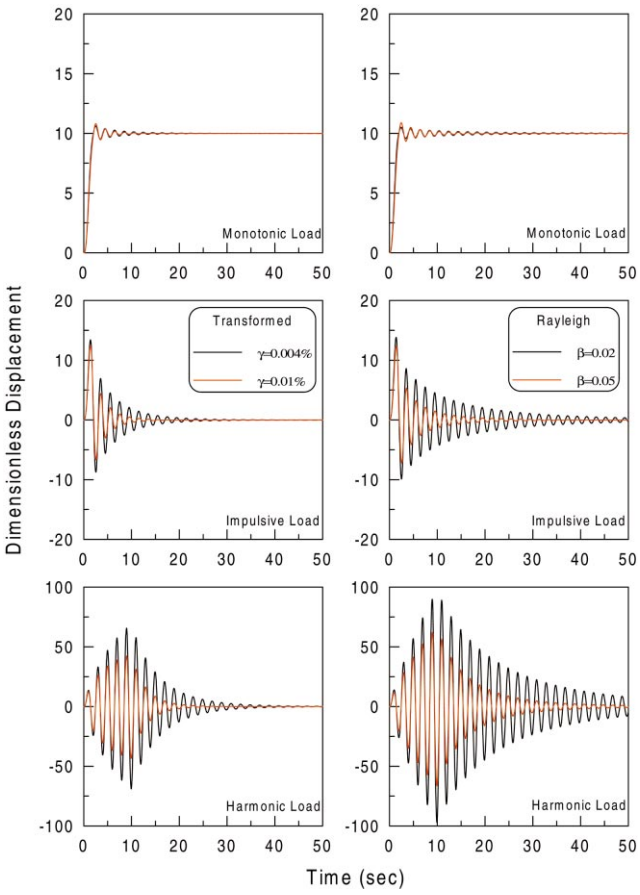

Fig. 10. Comparative SDOF structural response ($T_d = 1.98$ s $= T_n$).

transformed damping tends to reduce the response. When $T_n = T_d$, both solutions will get insignificant oscillations of the structural response under monotonic load; the Rayleigh solution provides much larger resonant displacement under the steady-state load. On the other hand, the suggested damping will reduce the free motions at the impulse. In the cases where the natural period of the structure is less than T_d, the oscillation of the displacement becomes much smaller, which yields more acceptable solutions. The free-motions of the structure reveal again the damping influences of the solutions. The higher damping suggested could reduce the response, in which the oscillations will decrease and decay faster than those predicted by Rayleigh damping. The proposed higher damping is mainly because the higher damping ratios (>5%) are encountered at relatively high frequencies (see Fig. 6), and they will certainly influence the transformed damping. On the other hand, the simplified Rayleigh damping adopts constant damping ratios (2 and 5%) for the whole frequency range of structural response. It is obvious that the proposed model would capture closely the importance of the frequency effects on damping for the time-domain structural analysis.

4. Summary

A time-dependent damping model is introduced in this paper. Fourier transforms and the impulse–response method are considered in establishing the model. To compute the equivalent damping ratios for the excitations, frequency-dependent damping ratios, modeled from the structural impedance functions or from experimental observations of the materials, are first obtained. These ratios are then incorporated with structural stiffness and the operational frequencies to calculate the transfer damping function. For simplicity, a Power function is suggested to fit the modeled ratios of the damping and the frequencies. By assuming symmetry of this function, a Power function, dependent on the structural stiffness and decaying with time, is again obtainable. As was noted, the resolved functional will remain positive as long as the order of the power spectrum is greater than -1.0. Procedures to obtain the model parameters are further discussed for the radiation damping of a single pile with the structural impedance functions and the material damping of Ottawa sand from cyclic torsional tests. By comparing the model solutions with those from Rayleigh damping

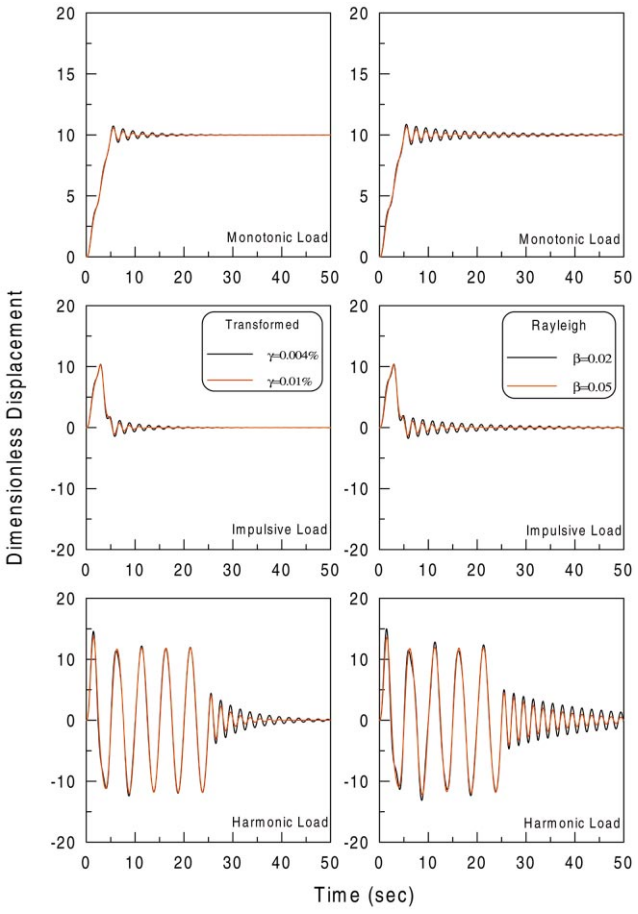

Fig. 11. Comparative SDOF structural response ($T_d = 5$ s $> T_n$).

for the response of a SDOF structure, this model is found amenable to time integration analysis, providing that the transform mathematics is fully satisfied.

References

[1] Bishop RED. The treatment of damping forces in vibration theory. Journal of the Royal Aeronautical Society 1955;59:738–42.
[2] Christian JT, Roesset JM, Desai CS. Two- and three-dimensional dynamic analyses. In: Desai CS, Christian JT, editors. Numerical methods in geotechnical engineering, 1977. p. 683–718 (chap. 20).
[3] Nashif AD, Jones IG, Henderson JP. Vibration damping. New York: Wiley, 1985.
[4] Schmidt LC. Vibration theory. In: Moore PJ, editor. Analysis and design of foundations for vibrations, Rotterdam, The Netherlands: A.A. Balkema, 1985. p. 21–63.
[5] Roesset JM. A review of soil–structure interaction. Seismic Safety Margins Research Program Project III — Soil–Structure Interaction, Research Report No. UCRL-15262. Lawrence Livermore Laboratory, 1980.
[6] Makris N, Constantinous MC. Application of fractional calculus in modeling viscous damper. In: SECED, editor. Earthquake, blast and impact-measurement and effects of vibration, Amsterdam: Elsevier, 1991. p. 151–62.
[7] Kagawa T. Dynamic soil reaction to axially loaded piles. Journal of Geotechnical Engineering, ASCE 1991;117(7):1001–20.
[8] Chen LY, Chen JT, Chen CH, Hong HK. Free vibration of a SDOF system with hysteretic damping. Mechanics Research Communications 1994;21(6):599–604.
[9] Inaudi JA, Kelly JM. Linear hysteretic damping and the Hilbert transform. Journal of Engineering Mechanics, ASCE 1995;121(5):626–32.
[10] Chang DW, Yeh SH. Time-domain wave equation analysis of single piles utilizing transformed radiation damping. Soils and Foundations, JGS 1999;39(2):31–44.
[11] Novak M. Dynamic stiffness and damping of piles. Canadian Geotechnical Journal 1974;11:574–98.
[12] Wolfram Research, Inc., Mathematica User Manual, Version 2.2. 1995.
[13] Roesset JM, Kausel E. Structural dynamics: notes on numerical integration methods. Department. of Civil Engineering, MIT, 1977.
[14] Chang DW, Ou Yang JF. Time-domain wave equation analysis with rational soil stiffness and damping coefficients in modeling axial pile response. In: Proceedings of the 13th Southeast Asian Geotechnical Conference, Taiwan, 1998. p. 777–81.
[15] Chang DW, Lin KC. Interaction effect on vertical pile response from time-domain wave equation analysis. In: Proceedings of the 2nd Earthquake Geotechnical Engineering Conference, Lisbon, Portugal, vol. 1, 1999. p. 407–12.
[16] Czajkowski RL, Vinson TS. Dynamic properties of frozen silt under cyclic loading. Journal of Geotechnical Engineering, ASCE 1980;106(GT9):963–80.
[17] Isenhower WM, Stokoe KH. Strain-rate dependent shear modulus of San Francisco Bay mud. In: Proceedings of the International Conference in Recent Advances in Geotechnical Earthquake Engineering and Soil Dynamics, vol. 2, 1981. p. 104–10.
[18] Sousa JB, Monismith CL. Dynamic response of paving materials. Transportation Research Record 1988;1136:57–68.
[19] Lin ML, Huang TH, You JC. The effects of frequency on damping properties of sand. Soil Dynamics and Earthquake Engineering 1996;15:269–78.
[20] Bray JD, Riemer MF, Gookin WB. On the dynamic characterization of soils. In: Proceedings of the 2nd Earthquake Geotechnical Engineering Conference, Lisbon, Portugal, vol. 3, 1999. p. 847–56.